

Efficient Algorithms for Locata Navigation Receiver Sensitivity Improvement

Faisal A. Khan, Andrew Dempster, Chris Rizos
The University of New South Wales

Abstract

Locata is a terrestrial position system that offers cm-level accuracies. Acquisition of degraded quality signals has always been a challenging task for radio navigation receivers and Locata is no exception. Locata's use of pseudorandomly gated CDMA signals further exacerbates the situation. This paper proposes four algorithms that offer improved signal acquisition in challenging situations and evaluates the performance of these algorithms in detail using real Locata signals. First, appreciating the complexity involved in the non-coherent acquisition of Locata signals, an algorithm is presented that exploits the inherent characteristics of the Locata gating sequence and offers receiver sensitivity improvement of around 1.3dB each time the integration duration is doubled. A concept of *assisted* acquisition is then introduced. It is shown that acquisition of any one signal can assist acquisition of the rest allowing reduction in mean acquisition time (MAT) and computational load and offering a further improvement of 1.7dB over previous algorithms. Next the use of long replica codes is suggested so as to allow for coherent integration. It is shown that this offers comparable sensitivity improvement and doesn't require any assistance. Finally an integrated scheme is described that employs the above-mentioned algorithms, and offers a signal acquisition approach better than the conventional one.

Keywords: Weak signal acquisition, interference mitigation, TH/DS-CDMA, acquisition performance improvement.

1. Introduction

Global Navigation Satellite Systems (GNSS) cannot always be relied upon, particularly indoors or in challenging signal environments. Locata is a position technology that offers cm-level accuracies in difficult positioning environments by complementing and sometimes even replacing GNSS. It employs time-synchronised terrestrial transceivers (called LocataLites)

transmitting time-multiplexed pulsed-CDMA signals in the licence-free ISM band. Operation in the ISM band permits signal transmission at much higher power levels than those received from GPS, and avoids any licence requirement. However, operation in the licence-free ISM band is vulnerable to interference from other devices using the same spectral band. It is likely that a larger number of devices operate in this band than any other licensed band. These interfering devices artificially elevate the noise floor in this band, degrading Locata's signal-to-noise- and interference-ratio (SNIR). (Khan *et al.*, 2010), using real data, identifies that Locata operation degrades in the presence of such noise and interference. This situation affects signal acquisition more than the tracking process, as it is relatively less immune to the received noise and interference. This paper proposes four algorithms that exploit the Locata system and signal architecture and characteristics to improve signal acquisition in such situations.

Locata employs a pulsed CDMA (time-hopped CDMA - TH/DS-CDMA) architecture to avoid the near-far issue. Locata pulsing is shown in Figure 1. TH/DS-CDMA is a gated version of a continuous DS-CDMA signal where gating is performed using a memory-based pseudorandom sequence. This allows a TDMA scheme to be employed by the LocataLites, using a multi-slot frame, where each LocataLite is assigned a single slot for transmission. This slot allocation is based on the pseudorandom gating sequence. The slot allocation sequence repeats after every 200 frames, where each frame is 1ms long and contains 10 slots of 0.1ms duration each. With a data rate of 50bps, each frame is modulated by 10 navigation data bits, where the bit boundaries are aligned with the slot boundaries. Each LocataLite employs two transmit antennas (A1 and A6), with each antenna transmitting at each of the two carrier frequencies (S1 and S6). This allows the Locata receiver to track four signals (A1S1, A1S6, A2S1 and A2S6) from each LocataLite. All four signals from a LocataLite are transmitted simultaneously in the same slot. LocataLites operate in a master-slave architecture where all slave LocataLites are time-synchronised with the master. This time-synchronization (known as *TimeLoc* -

Barnes *et al.*, 2003) allows the LocataLites to align the start of the transmitted PRN code with the start of their allocated slot (Cheong *et al.*, 2010).

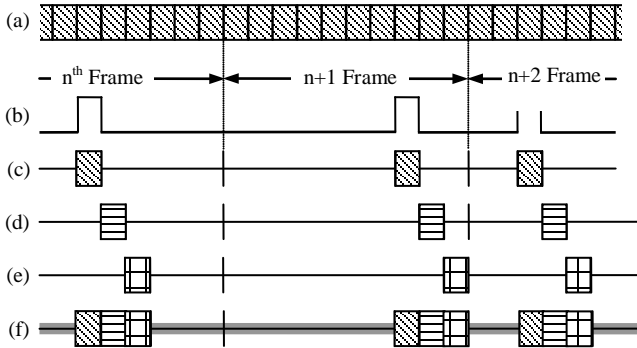


Figure 1: (a) Continuous DS-CDMA Signal from LocataLite 1, (b) Slot Allocation Sequence (SAS), (c) Pulsed CDMA (TH/DS-CDMA) for LocataLite 1 obtained by gating (a) with (b), (d) Pulsed CDMA (TH/DS-CDMA) for LocataLite 2 allocated slots subsequent to LocataLite 1, (e) Pulsed CDMA (TH/DS-CDMA) for LocataLite 3 allocated slots subsequent to LocataLite 2, (f) Received signal including noise.

A promising solution that facilitates weak signal acquisition in GNSS receivers is increasing the integration time (coherently or non-coherently) during the acquisition process (Borio *et al.*, 2008). However, in contrast to GNSS where received signals are continuous in nature, use of pulsed CDMA makes coherent integration exceedingly complex and non-coherent integration more complicated than for GNSS. This is mainly due to the pseudorandom nature of the pulsing sequence. In addition, the discontinuous nature of the Locata signal also adds to the problem, increasing the computational load as well as the mean acquisition time (MAT).

This paper identifies that if this pulsing sequence is arranged in a certain manner, its inherent characteristics can be exploited to achieve improved integration gains. A Probabilistic Non-Coherent Acquisition (PNCA) algorithm is proposed to integrate the signal using the probability of pulse occurrence. It is shown that the PNCA algorithm offers an acquisition sensitivity improvement by non-coherently extending the integration duration over multiple code periods.

Although non-coherent integration over multiple code periods improves the probability of detection (P_D), it also increases the MAT. It needs to be appreciated that this increase can be substantial, particularly due to the time-multiplexed nature of the Locata signal. Again by exploiting the Locata slot allocation scheme and the fact that all the LocataLites are time-synchronised,

information gained from the first acquired signal can be used to reduce the computational load, as well as to further improve the acquisition of weak/low CNIR (carrier-to-noise- and interference-ratio) signals from the same as well as the other LocataLites. A new concept of *Assisted Start* is introduced, falling under a similar classification as *hot*, *warm* and *cold* starts. This is shown to help in situations where signals at one of the frequencies are degraded by received interference. Acquisition of a signal at the least affected frequency can be prioritised in such cases thereby eliminating the requirement of acquiring the degraded signals i.e. the tracking of those degraded signals can commence without them being “acquired”. It is shown that *assisted start* does not need prior knowledge required by hot/warm starts in case of GNSS.

The PNCA algorithm enables an extension of the integration duration in a non-coherent manner. Alternatively, Assisted Acquisition allows coherent integration but requires prior acquisition of at least one signal. An algorithm is suggested based on long replica codes that facilitates coherent integration without any prior signal acquisition requirement. It is shown that this algorithm outperforms the PNCA algorithm in terms of sensitivity improvement but at some extra cost.

Based upon the proposed algorithms, an overall Locata signal acquisition strategy is suggested. It is shown that the information related to the received noise and interference, gained from the acquisition of signals from one LocataLite, can help to assist acquisition of signals from other LocataLites. This overall strategy offers reduced processing load, improved receiver sensitivity (better acquisition of weak/low CNIR signals), lower MAT and eventually a shorter time to first fix (TTFF).

The novel contributions of this paper are as follows:

1. Proposal of a Probabilistic Non-Coherent Acquisition (PNCA) algorithm and a Long Replica Code Acquisition (LRCA) algorithm offering extension of integration duration beyond the single code period, allowing improved acquisition of weak/low CNIR signals and hence improved receiver sensitivity.
2. Proposal of *Assisted* acquisition algorithms that offer reduction in processing load as well as in the mean acquisition time.

It is shown that using the assisted acquisition algorithms, no reacquisition of *lost* signals from a LocataLite is required as long as one of the signals from that LocataLite is still being tracked. After introducing the theme of the paper in this section, the acquisition algorithms are presented, analyzed and evaluated in the subsequent sections.

2. Probabilistic Non-Coherent Acquisition (PNCA)

Although the use of TH/DS-CDMA helps alleviating the near-far issue (Cobb, 1997), it causes the received signal to be discontinuous, making it more complicated to integrate over multiple code periods. This can be explained as follows: Each LocataLite transmits during a pseudorandomly allocated slot in a 10-slot frame. This adds a third dimension to the acquisition search space: the position of the signal-containing-slot (SCS) in the received frame, in addition to the two dimensions more familiar from GNSS: the received signal's code-phase and carrier Doppler. For acquiring weak or low SNIR signals, if the receiver is intended to perform integration over multiple code periods, no information is available about the position of the desired SCS in subsequent frames that can be used to combine energy for improved acquisition. The position of the SCS in the received frame is defined by the element s with index k in the slot allocation sequence S .

A straightforward approach for combining the energy in the received signal (containing both desired and undesired slots) can involve integration over the entire duration of n frames. This offers the advantage in terms of potentially reduced complexity, as no effort is invested in searching for the desired SCS. However such integration over the entire set of frames would accumulate more noise power. This is due to the fact that only 10% of the slots in the considered frames contain the desired signal and the energy from the rest of the slots contributes towards noise. This will eventually result in SNIR reduction by at least 10dB.

The algorithm presented in this section uses the probable positions of SCSs to integrate over multiple code periods for determining all three acquisition parameters for low SNIR signals.

All the manuscripts should be submitted in English. In the preparation of the manuscripts, authors are expected to pay attention to both scientific accuracy and clarity of presentation for their work.

2.1 Algorithm

Locata's pseudorandom slot allocation sequence can be represented as a 200 element vector S , where

$$S = \{s_1, s_2, s_3, s_4, \dots, s_k, \dots, s_{199}, s_{200}\} \quad (1)$$

here s_k ($2 \leq s_k \leq 19$) defines the SCS with index k in S . A hopping sequence vector H can then be defined as:

$$H = \{h_1, h_2, h_3, h_4, \dots, h_k, \dots, h_{199}, h_{200}\} \quad (2)$$

where

$$h_k = s_k - s_{k-1} + 10 \quad \forall s_k \in S \quad (3)$$

Here a "hop" is defined as one plus the number of slots occurring between two consecutive slots containing the desired signal (SCS) as depicted in Figure 2(a). The vector H suggests that if the position of an SCS from a LocataLite in a received frame is known (say m) then the SCSs from that LocataLite in the subsequent frames will be present at $m + h_1, m + h_1 + h_2, \dots$ slots, as depicted in Figure 2(b). This vector H can be rearranged to form a 20×10 matrix H_{M_1} given as:

$$H_{M_1} = \begin{bmatrix} h_1 & h_{21} & h_{41} & \dots & \dots & h_{181} \\ h_2 & h_{22} & & & & \vdots \\ h_3 & \vdots & \ddots & & & \vdots \\ \vdots & \vdots & & \ddots & & \vdots \\ \vdots & \vdots & & & \ddots & h_{199} \\ h_{20} & h_{40} & \dots & \dots & h_{180} & h_{200} \end{bmatrix} \quad (4)$$

Finally, a matrix H_{CM_1} can be defined with elements h_{cm_1} (i th element of the j th column) representing the sum of the first i elements in the j th column of H_M :

$$h_{CM_{ij}} = \sum_{x=1}^i h_{20 \times (j-1) + x} \quad (5)$$

Using Locata slot allocation sequence S (Cheong et al., 2010), an H_{CM_1} matrix is generated and is given in

Equation (6):

$$H_{CM_1} = \begin{bmatrix} 8 & 18 & 8 & 8 & 8 & 8 & 18 & 8 & 8 & 8 \\ 22 & 22 & 12 & 22 & 12 & 22 & 22 & 22 & 22 & 22 \\ 33 & 43 & 33 & 43 & 33 & 43 & 43 & 43 & 43 & 43 \\ 47 & 57 & 47 & 47 & 47 & & \ddots & & \ddots & 47 \\ 55 & 65 & 55 & 65 & & & & \ddots & & 55 \\ & & \ddots & & \ddots & & & & \ddots & \vdots \\ & & & & & & & & \dots & 202 \end{bmatrix} \quad (6)$$

H_{CM_1} suggests that if the desired SCS in the received signal was s_k (say $k=1$), then the subsequent SCSs ($s_2, s_3, s_4 \dots$) will be present at positions $k+8, k+22, k+26$ and so on. Similarly, if the desired SCS in the received signal was s_k ($k=21$), then the subsequent SCSs ($s_{22}, s_{23}, s_{24} \dots$) will be present at positions $k+18, k+22, k+36$ and so on. The reason for formulating the 20×10 structure for H_{CM_1} becomes clear by noting that each row in H_{CM_1} contains only two numbers, obtained due to the inherent characteristic of S . Assuming that the position

of a slot is known (say m) which is an SCS ($s'_k \in \{1, 21,$

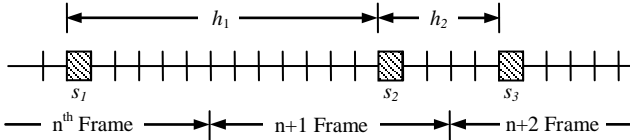


Figure 2(a)

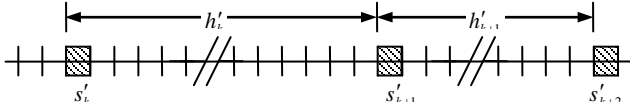


Figure 2(b)

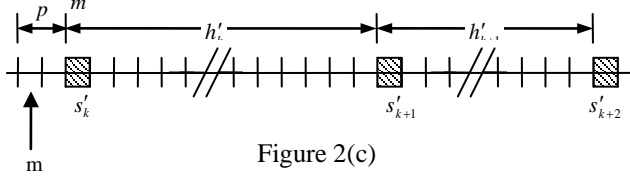


Figure 2(c)

Figure 2: Locata Slot Allocation

41, 61, 81, 101, 121, 141, 161, 181}), H_{CM_1} suggests that the next SCS i.e. $s'_{k+1} \in \{2, 22, 42, 62, 82, 102, 122, 142, 162, 182\}$ will be present either at position $m+8$ (say m_8) (with 80% probability) or at m_{18} (with 20% probability). Similarly $s'_{k+2} \in \{3, 23, 43, 63, 83, 103, 123, 143, 163, 183\}$ will be present either at m_{22} (with 80% probability) or at m_{12} (with 20% probability), $s'_{k+3} \in \{4, 24, 44, 64, 84, 104, 124, 144, 164, 184\}$ will be present either at m_{33} (with 30% probability) or at m_{43} (with 70% probability), and so on. This suggests that the position of any subsequent SCS can be determined with a particular probability. Considering the probability of occurrence of an SCS at a given position, energy from multiple SCS can be combined using the following template:

$$T_1 = m + [0.8m_8 + 0.2m_{18}] + [0.8m_{22} + 0.2m_{12}] + [0.6m_{26} + 0.4m_{36}] + [0.7m_{43} + 0.3m_{33}] + [0.7m_{47} + 0.3m_{57}] + [0.5m_{45} + 0.5m_{55}] + \dots \quad (7)$$

The number of terms to be considered would be equal to the number of SCS intended for integration. The result of this integration is termed as primary integration I_{P_1} .

Note that the first slot considered (m) was assumed to be an SCS, as shown in Figure 2(b). If m was selected as shown in Figure 2(c), then to non-coherently integrate over the slots containing the desired signal, the above template would need to be delayed by p slots to align m with s'_k . This delayed template can be given as:

$$T_1 = m_p + [0.8m_{8+p} + 0.2m_{18+p}] + [0.8m_{22+p} + 0.2m_{12+p}] + [0.6m_{26+p} + 0.4m_{36+p}] + [0.7m_{43+p} + 0.3m_{33+p}] + [0.7m_{47+p} + 0.3m_{57+p}] + [0.5m_{45+p} + 0.5m_{55+p}] + \dots \quad (8)$$

Where

$$\begin{aligned} m_p &= m+p \\ m_{q+p} &= m+q+p \end{aligned} \quad (9)$$

This suggests that, to perform successful acquisition, a sliding search needs to be performed to align m with s'_k , over the range $0 \leq p \leq \max(R_{H_{CM}})^l$, where $R_{H_{CM}}$ denotes the first row of H_{CM} . Note that m_p will be the position of the first SCS in the received signal. Also note that H_{CM_1} was obtained by considering h_1 as the first element of H_{M_1} . A different H_{CM} would be obtained by considering h_2 as the first element of H_M as follows:

$$H_{M_2} = \begin{bmatrix} h_2 & h_{22} & h_{42} & \dots & \dots & h_{182} \\ h_3 & h_{23} & & & & \vdots \\ h_4 & \vdots & \ddots & & & \vdots \\ \vdots & \vdots & & \ddots & & \vdots \\ \vdots & \vdots & & & \ddots & h_{200} \\ h_{21} & h_{41} & \dots & \dots & h_{181} & h_1 \end{bmatrix} \quad (10)$$

A similar procedure can be employed to obtain the new H_{CM} and consequently the template T as the previous H_{CM_1} and T_1 . It is to be noted that a total of 20 templates need to be generated, (starting from $h_1 - h_{20}$) after which the $H_{CM_1} - H_{CM_{20}}$ (and the templates) will start repeating.

The probabilistic non-coherent integration acquisition (PNCA) algorithm can now be summarised as follows:

1. Selecting $h_1 - h_{20}$ as the starting points, generate the corresponding HM and HCM matrices, and the resulting templates T .
2. Select an integration duration.
3. Set the template delay as zero.
4. Generate correlator outputs.
5. Compute the primary integration results $I_{P_1} - I_{P_{20}}$ by using the templates $T_1 - T_{20}$.
6. Select the primary integration result I_P that generates the highest peak, and check whether the obtained peak has crossed the acquisition threshold V_t .
7. If the peak has crossed the threshold, declare acquisition of code phase and carrier Doppler.
8. If the peak has not crossed the threshold, delay all the templates by one slot and repeat from step 4.

9. If all the delays have been exhausted for the generated templates, increase the integration duration and repeat from step 3.
10. If maximum integration duration is reached, and the peak hasn't crossed the threshold, move on to the next cell (the next Doppler step).

The above primary integration considers probable SCS positions to obtain acquisition peak using the H_M and H_{CM} matrices. These matrices can also be used to determine the index k of the first SCS in the received signal, and thus the exact positions of the subsequent SCSs. Say during primary integration T_1 , after being delayed q slots, generates the highest correlation peak that crosses the threshold. This indicates that one of the columns of H_{M_1} correctly describes the hopping sequence of SCS in the received signal. In other words, the SCS in the received signal can be present at either $\{m_q, m_{8+q}, m_{22+q}, m_{33+q}, m_{47+q}, m_{55+q}, \dots\}$ or $\{m_q, m_{18+q}, m_{22+q}, m_{43+q}, m_{57+q}, m_{65+q}, \dots\}$ and so on. The task here is to identify the column indicating the correct SCS positions. Once this column is identified, the first element of that column will indicate the hop between the first two SCS in the received signal. Note that the index of the first hop will be the index of the first SCS in the received signal. This is because by definition (Equation 3), the index k of hop h (in H) is same as the index of the preceding SCS s (in S). To identify this column, secondary integrations $I_{S_1} - I_{S_{10}}$ need to be performed using the hops from each of the columns, as follows:

$$I_{S_1} = m_q + m_{8+q} + m_{22+q} + m_{33+q} + m_{47+q} + m_{55+q} + \dots$$

$$I_{S_2} = m_q + m_{18+q} + m_{22+q} + m_{43+q} + m_{57+q} + m_{65+q} + \dots$$

$I_{S_3} = m_q + m_{8+q} + m_{12+q} + m_{33+q} + m_{47+q} + m_{65+q} + \dots$, and so on.

The correct column can then simply be identified by considering the secondary integrating producing the highest correlation value. It is to be noted that secondary integration considers only one H_M . This potentially reduces the computational load in contrast to primary integration (that considered 20 H_M) making it feasible to integrate over individual H_M columns.

2.2 Implementation Results

In order to validate the proposed PNCA algorithm real Locata IF samples were collected using a National Instruments PXI 5142 digitiser. These samples were collected wirelessly, which allowed introduction of multipath effects. In order to collect high SNIR signals, the LocataLite was set to transmit at the highest possible power level. The wide band noise with a Gaussian distribution was later added artificially (within Matlab). This was done in order to achieve desired CNIR levels, and to conduct the experiments in a controlled and

repeatable environment so that the performance statistics can be generated.

First, in order to establish a baseline situation, Locata signal acquisition was attempted using the conventional approach, i.e. by integrating over a single code period. Figure 3 shows the implementation results in terms of probability of detection (P_D) plotted against CNIR. A P_D above 90% for a $P_{fa} = 1 \times 10^{-3}$ was considered good enough to declare successful acquisition. According to Figure 3, for the integration over a single code period, this was achieved with a minimum CNIR of 53.48dB-Hz. It is interesting to note that this value is roughly 10dB more than that which can be expected for the GPS L1 signal (Kaplan & Hegarty, 2005). This is mainly due to the wider bandwidth (10 times wider than GPS L1 signal due to the higher chipping rate) of the Locata signals.

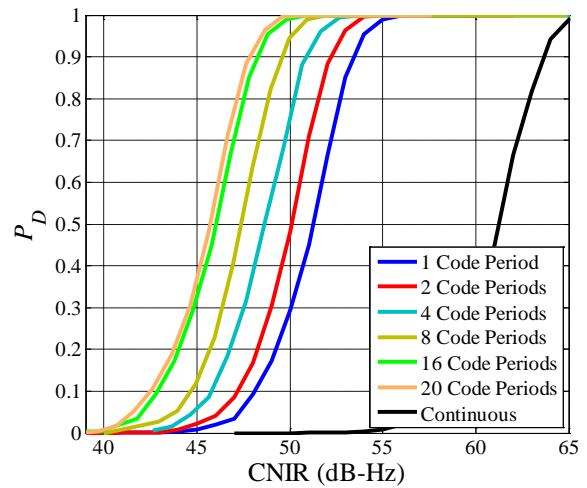


Figure 3: PNCA algorithm performance offering non-coherent integration over multiple code periods. Results for single code period acquisition and continuous integration (over 20 code periods) are also plotted for comparison.

Also plotted in this figure for comparison are the results for continuous integration over the entire frame. It can be noted that in this case the situation was even worse than the case of single code period integration as the desired P_D was achieved at a CNIR of 63.5dB-Hz. This was in accordance with the discussion presented above.

The acquisition results, obtained using PNCA algorithm, are also plotted in this figure. These results show that as the integration duration was extended to cover two periods, the signal acquisition was achievable at 52.2dB-Hz; a margin of around 1.3dB improvement as compared to the previous case. It can be seen that with integration over 20 code periods, a total margin of 5.5dB was obtained. Note that if the hop duration was known (the equivalent of coherent integration in CDMA), integration of 20 periods would lead to a gain of 13dB.

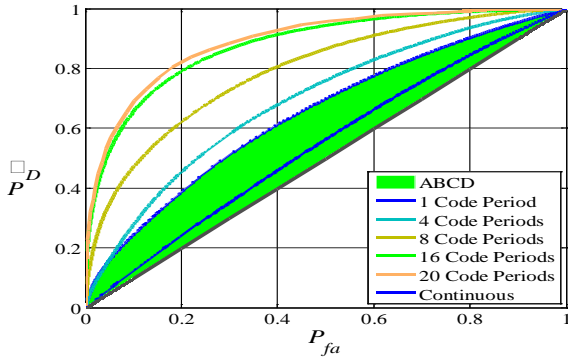


Figure 4: ROC curves obtained using PNCA algorithm and continuous integration. Dotted line

To analyse the situation from another dimension, receiver operating characteristic (ROC) curves are plotted for the proposed scheme in Figure 4. A low CNIR value of 42dB-Hz is chosen, as this is a CNIR level where signal acquisition is difficult with integration over a single code period, as shown in Figure 3. It can be noticed from Figure 4 that the PNCA algorithm effectively identifies the SCS positions and improves the probability of detection by extending the integration duration beyond a single code period. Also plotted in this figure is the ROC curve for the continuous integration approach where integration was performed over the entire 20 frames. This curve suggests that the integration over entire frames (continuous integration) is futile as the ROC curve moves closer to the diagonal. This was mainly due to the noise accumulation during this process, as discussed above.

A rule-of-thumb for the ROC curves can be stated as: a curve closer to the north-west corner is more desirable than one closer to the diagonal (benefit-to-cost ratio ($\frac{P_D}{P_{fa}}$) of 1). In other words, the greater the *area between the curve and the diagonal* (ABCD), the better will be the performance. This area, marked in green on Figure 4, also shows how much of the population of one set of outcomes (false alarms) is distinguishable from the other (correct detections). It may be noted that two curves with similar ABCD may not always indicate similar performance for two different algorithms, or changes in characteristics. However, as all the curves depicted here are symmetric to the other diagonal, a larger ABCD does signify better performance. Figure 4 illustrates how the extension of the integration duration using the PNCA algorithm improves the benefit-to-cost ratio, as depicted by the increase in the corresponding ABCD. It can also be observed that the situation with continuous integration gets worse, as the curve moves much closer to the diagonal, reducing the corresponding ABCD.

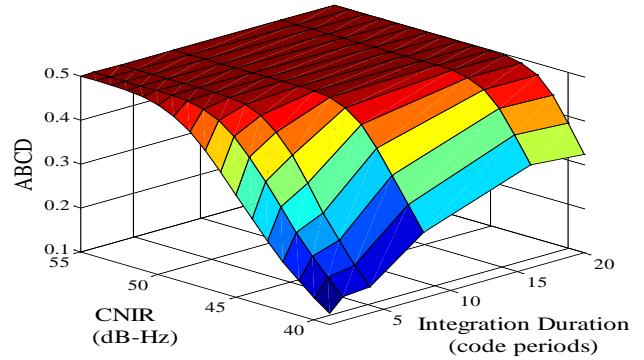


Figure 5: Area between the ROC curves and the diagonal (ABCD) obtained using PNCA algorithm.

Similar curves can be plotted for any other CNIR level. However, it can be confusing to plot all the curves for the desired range of CNIR values and integration durations on the same figure for comparison purposes. To simplify as well as to summarise the situation, ABCD can be chosen as a comparison metric here based on the above discussion. Figure 5 shows the ABCD values for different integration durations over a range of CNIR values. This figure clearly shows that the PNCA algorithm offers performance improvement even at lower CNIR values by successfully increasing the integration durations. The term *successful* is used here to refer to the fact that the PNCA algorithm identified the SCS positions with a higher probability resulting in improved performance, in contrast to continuous integration approach where no SCS identification is performed.

An important trade-off in the acquisition process is that of MAT against receiver sensitivity. Longer integrations beyond a single code period offer improved receiver sensitivity, however at the cost of increased MAT. This is evident from Figure 6, where MAT curves for the PNCA algorithm are plotted for different integration durations. MAT values plotted here were calculated considering a search space of 20460 code delays using a 0.5 code step for ten code periods of 1023 chips each. Ten code periods were considered for the code dimension as the whole frame (10 code periods long) needs to be searched to determine the code start. In addition, 41 frequency bins were considered using a bin size of 500Hz to cover a Doppler search space of ± 10 KHz. The penalty factor K was set to be $\frac{1}{\tau_D}$ (Holmes, 2007). This figure indicates that the smaller integration durations offer lower MAT for high CNIR signals. However, as the CNIR decreases, MAT for smaller integration increases rapidly due to an increase in the number of false alarms (reflected by increased P_{fa}). This is overcome by extending the non-coherent integration duration by using the PNCA algorithm. This results in increasing P_D and consequently a lower MAT.

This figure also suggests that if the information about the noise present in the received signal is known *a priori*, a larger integration duration can be used directly, instead of initially trying smaller integration durations.

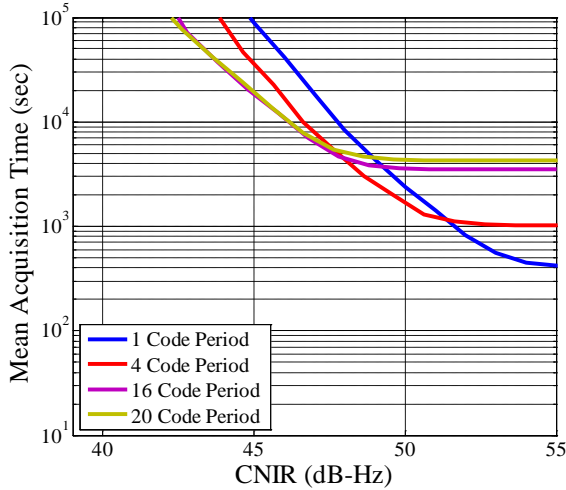


Figure 6: Mean acquisition time achieved using PNCA algorithm for different non-coherent integration durations.

3. Assisted Acquisition

In GNSS, concepts of *warm* and *hot* start are commonly used, where prior information including but not limited to the last calculated position, satellites in view, last used almanac and UTC time can be used to facilitate faster signal acquisition. Both of these approaches are equally applicable to Locata signal acquisition. In addition, a new term “assisted start” is introduced here. In contrast to the two types of *start* listed above, no information related to the last calculated position and/or last used almanac is required. In an *assisted* start, information gained from the first acquired signal from any of the LocataLites is used to achieve faster acquisition with reduced computational load for other signals from the same as well as the other LocataLites. A significant advantage that *assisted* acquisition offers is the improved acquisition of weak/low SNIR signals. Information required for assisted start may include position of slot boundaries, SCS index, code start (CS) and carrier-Doppler (CD). Assisted acquisition can be categorised as follows:

1. Assisted Acquisition-I (AA-I): Using code start and carrier-Doppler from the first signal, the same can be determined for the rest of the signals from the same LocataLite.
2. Assisted Acquisition-II (AA-II): Using SCS index, and slot boundary related information obtained by acquiring first signal from any LocataLite helps improved acquisition of the signals from the rest of the LocataLites, allowing non-coherent as well as coherent integration over multiple code periods.

These are discussed in detail below:

3.1 Assisted Acquisition-I (AA-I)

The AA-I approach offers reduction in computational load and MAT by acquiring only one signal per LocataLite and generating the acquisition parameters for the rest of the signals from that LocataLite. In addition, it offers direct tracking for signals affected by received noise and interference, for which acquisition were not possible. This is achieved by exploiting the fact that *the minimum CNIR required for tracking is less than that required for acquisition*.

Table 1 – Relationships for determining acquisition parameters for signals from same LocataLite.

Acquisition Parameter	Description
CS_{A1S1}	Considered as being already acquired.
CD_{A1S1}	Considered as being already acquired.
$CS_{A1S6} = CS_{A1S1}$ $CS_{A2S6} = CS_{A2S1}$	As both the codes originate from the same transmit antenna and terminate at the same receive antenna. Also all the PRN codes from a LocataLite are aligned with the slot start.
$CD_{A1S6} = R \times CD_{A1S1}$ $CD_{A2S6} = R \times CD_{A2S1}$	As both A1S1 and A1S6 originate from the same transmit antenna, the Doppler will differ only by the ratio of the two carrier frequencies.
$CS_{A2S1} \approx CS_{A1S1}$	Both codes originate from two different transmit antennas typically placed up to 1 metre apart. This may contribute towards a maximum misalignment of 0.03 chips in the CS of the two codes, which can be safely neglected for acquisition.
$CD_{A2S1} \approx CD_{A1S1}$	As both the signals originate from two different antennas, their direction vector (contributing towards Doppler) will be slightly different. However, the difference in Doppler due to this will be much smaller than the Doppler search step in the acquisition process, and can be covered during the pull-in process at the start of tracking.

Each LocataLite employs both of the two antennas (A1 and A2) to transmit on each of the two frequencies (S1 and S6), making a total of four signals being transmitted. In other words, the rover receiver acquires four signals

from each LocataLite. If the received noise and interference corrupts signals at either of the two frequencies, degrading their CNIR and making their acquisition difficult, acquisition parameters obtained externally can be used directly to commence tracking without these signals actually being “acquired”. Table 1 lists the relationships which can be used to obtain these acquisition parameters (CS and CD) for other the three signals (within close approximations), if one of the signals (say A1S1) has already been acquired. A similar approach has earlier been suggested for acquiring multiple components of the Galileo E5 signal. However, here it is exploited for four individual signals. Note that the third acquisition parameter (SCS index) remains the same for all four signals as all signals from the same LocataLite are transmitted in the same slot.

In order to validate the above discussion, Table 2 shows the values of the acquisition parameters for all of the four signals from the same LocataLite obtained using conventional acquisition approach. It can be seen that the acquired parameters are very similar to values estimated using relationships presented in Table 1.

Table 2 – Comparison of estimated and actually acquired acquisition parameters

Acquisition Parameter	Acquired Value	Estimated Value
CS _{A1S1}	7494	-
CD _{A1S1}	-1763	-
CS _{A2S1}	7494	7494
CD _{A2S1}	-1765	-1763
CS _{A1S6}	7494	7494
CD _{A1S6}	-1800	-1800
CS _{A2S6}	7494	7494
CD _{A2S6}	-1802	-1800

The synchronisation between the signals from the same LocataLite not only offers assistance in first time acquisition but can also offer assistance for any signal for which the tracking has been lost. No re-acquisition is required for such a signal as long as at least another signal from that LocataLite is still being tracked. Carrier-Doppler, position of code start, and the position of the SCS for the lost signal can be easily obtained from any of the tracked signals from the same LocataLite using the relationships in Table 1.

To further highlight the advantage offered by the AA-I approach, numerical noise was added to the signals at the S6 frequency to degrade their CNIR to 50dB-Hz. The

signals at the S1 frequency were unaffected. It was observed that, using an integration duration of a single code period, the acquisition was possible only for A1S1 could not be acquired. However, it was observed that the and A2S1 signals, while the A1S6 and A2S6 signals tracking could be easily triggered for these affected signals at the S6 frequency by using the acquisition parameters obtained from the A1S1 signal and the relationships presented in Table 1.

3.2 Assisted Acquisition-II (AA-II)

Although the PNCA algorithm offers improved acquisition performance for the first acquired LocataLite, AA-II offers further advantages for acquiring subsequent LocataLites. For Locata, three parameters: code start, carrier-Doppler and the SCS index, need to be determined to declare successful acquisition. As already mentioned, each LocataLite is allocated a single slot in a 10-slot frame. According to the Locata slot allocation scheme, the subsequent slots are allocated to the subsequent LocataLites (Cheong *et al.*, 2009a), as depicted in Figure 7. This suggests that the SCS index needs to be determined for only one of the LocataLites and the following slots can be taken as being assigned to the subsequent LocataLites. This allow, for acquiring subsequent LocataLites, an increase in integration duration to multiple code periods by considering the correct positions of the SCS instead of probable positions as in case of PNCA. Also the knowledge of SCS index can be used to determine data bit boundaries as these are aligned with SCS boundaries of known index. This facilitates the use of coherent integration over multiple code periods.

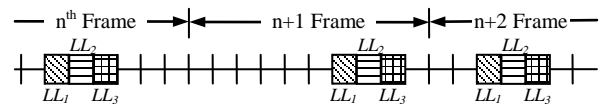


Figure 7: Locata Slot Allocation for consecutive LocataLites.

In addition, AA-II offers a reduction in search space requiring only a limited number of IF samples to be searched in order to determine the start of the PRN code in comparison to unassisted acquisition algorithms where a much larger number of IF samples need to be searched. The pulsed nature of the Locata signal requires a different approach for code acquisition as compared to the case of GPS signals, for instance. In the case of GPS, FFT-based acquisition exploits C/A code’s time continuity to employ circular convolution. This requires relatively fewer IF samples (covering few code periods’ duration) to be searched to acquire the PRN code’s *phase*, instead of searching for its *start*. However, in the case of Locata, where a gated (discontinuous) DS-CDMA signal is used, linear convolution needs to be performed to avoid losses due to circular convolution (Cheong *et al.*, 2009b). Due to the fact that each frame

contains only one desired SCS, IF samples covering the duration of multiple such frames need to be searched to find the code start. This suggests that ten times the number of IF samples need to be searched in the case of Locata than in case of GPS, as the frame duration is ten times the PRN code duration. However, if some prior information is available, then this search space can potentially be reduced. Thanks to TimeLoc, the start of a LocataLite's PRN code is aligned with the start of its allocated slot, as mentioned earlier. This allows slot boundaries to be determined with the acquisition of code start for any LocataLite and, in theory, eliminates the requirement for the search of rest of the LocataLites' code starts.

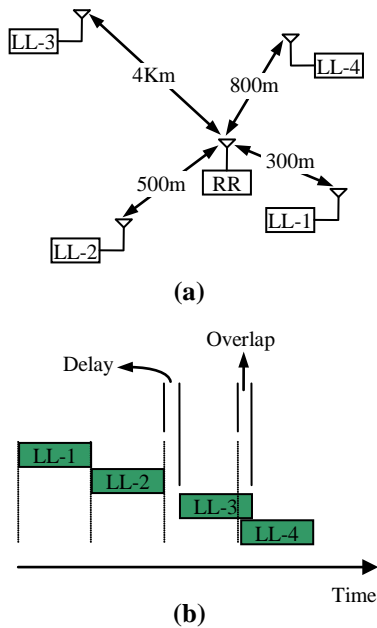


Figure 8: (a) Locata Network configuration Example, (b) Different LocataLites' signals as received by the rover receiver.

However, in a real world scenario, the situation could be little different. A scenario could be considered where the rover receiver and LocataLites are positioned as shown in Figure 8(a). Signals transmitted by different LocataLites, although all aligned with the slot boundaries at the time of transmission, reach the rover receiver with different delays (with respect to the actual slot boundaries) depending upon the receiver-LocataLite distance. This is depicted in Figure 8(b). This suggests that the start of a LocataLite's PRN code could either overlap (e.g. LL-3/LL-4) or be delayed (e.g. LL-2/LL-3) with respect to the end of the code in the previous slot. Considering 4km to be the transmission range of a LocataLite, a maximum difference of 4km can be assumed between distances from rover receiver to any two LocataLites. This distance will result in a maximum overlap/delay of $13.33\mu\text{s}$, or about 137 code chips

(considering Locata PRN code chipping rate of 10.23Mcps). This suggests that in practice, for detecting the start of a subsequent LocataLite's PRN code, the receiver needs to search only ± 137 chip delays from the finishing point of the previous PRN code, as compared to searching the whole frames. This not only reduces the computational burden but also improves the mean acquisition time (MAT).

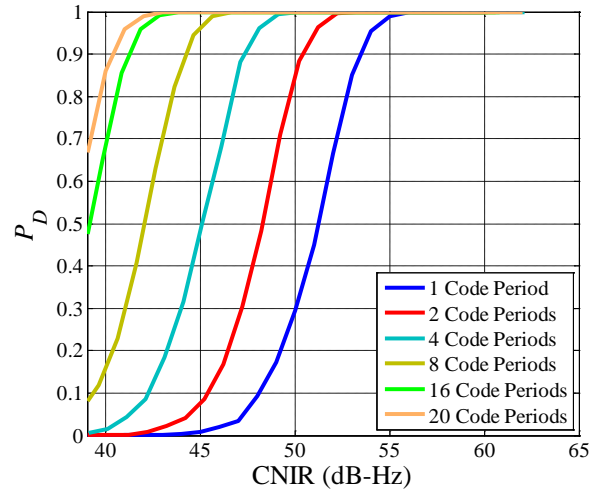


Figure 9: A-II algorithm performance offering non-coherent integration over single and multiple code periods.

To demonstrate the acquisition performance improvement offered by the AA-II algorithm P_D vs. CNIR curves are plotted in Figure 9 for different integration intervals. The same data as in section 2.2 was used to generate these curves. The curves in this figure are directly comparable with those plotted in Figure 3. It can be noticed that, for a given integration duration, the performance improves by 1.7dB as compared to the PNCA algorithm. This can be explained as follows: In the PNCA algorithm, energy is accumulated by considering the probable positions of SCS. As the SCS positions are not known with certainty, energy in each slot is integrated after being weighted according to the probability of that slot being an SCS. In the case where the considered slot is not an SCS, it contributes noise reducing the overall integration gain. Even if the considered slot actually is an SCS, an ideal weight of 1 still cannot be used due to the ambiguity involved. AA-II considers the correct slot positions that allow the use of unit weight for all the slots improving the overall integration gain.

Figure 10 shows the ROC curves plotted to analyse the benefit-to-cost ratio of the proposed algorithm. These curves are generated again for a CNIR value of 42dB-Hz and therefore are directly comparable to those of the PNCA algorithm in Figure 4. Significant improvement offered by the AA-II algorithm, as compared to the

PNCA algorithm for the considered integration durations, is again evident from these curves. It can be observed that for integrations over 16 code periods or more, the AA-II algorithm offers a 100% P_D for almost all of the values of P_{fa} . This suggests that the AA-II algorithm distinctly identifies the correct detections and minimises the overlap between the “correct detection” and “false alarm” distributions even at lower CNIR values.

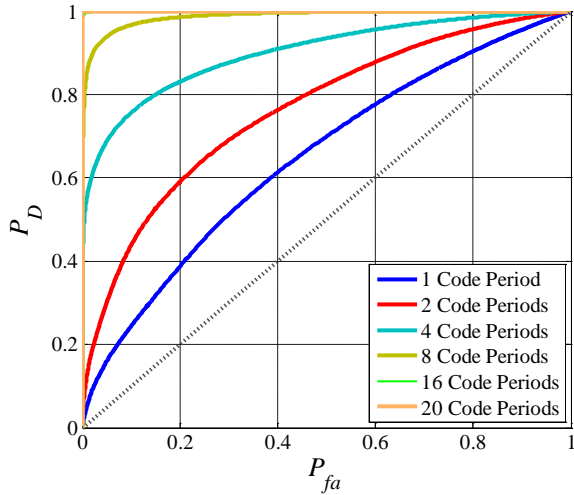


Figure 10: OC curves obtained using AA-II algorithm. Heavy Dotted line shows the diagonal.

Figure 11 shows the ABCD values achieved using the AA-II algorithm, which are again directly comparable to those for the PNCA algorithm. This figure again reinforces the previously made observation that for all CNIR values, the AA-II algorithm outperforms the PNCA algorithm for any given extension in integration duration. This figure also suggests that the AA-II algorithm offers a higher cost-to-benefit ratio even for the lowest considered CNIR value for any given value of P_{fa} as the integration duration increases. An interesting point to note here is that both the AA-II and the PNCA algorithms offer similar performance for high CNIR values by integrating over multiple code periods.

Considering the situation from another direction, the MAT curves for the coherent integration performed using the AA-II algorithm are plotted in Figure 12. Again, this figure is directly comparable with Figure 6. It can be seen that, for the same integration duration, the improved gains offered by coherent integration decreases the MAT as compared to non-coherent integration performed using the PNCA algorithm. Note that this decrease is also contributed by the reduction in the number of code delays to be searched, as these were reduced from 20460, in the case of PNCA algorithm, to 548. This was due to the fact that only ± 137 chips needed to be searched, as mentioned earlier. The difference in MAT due to this factor can be particularly

noticed from the curves obtained using 1 code period integration, as these did not include any effects of coherent/non-coherent integration.

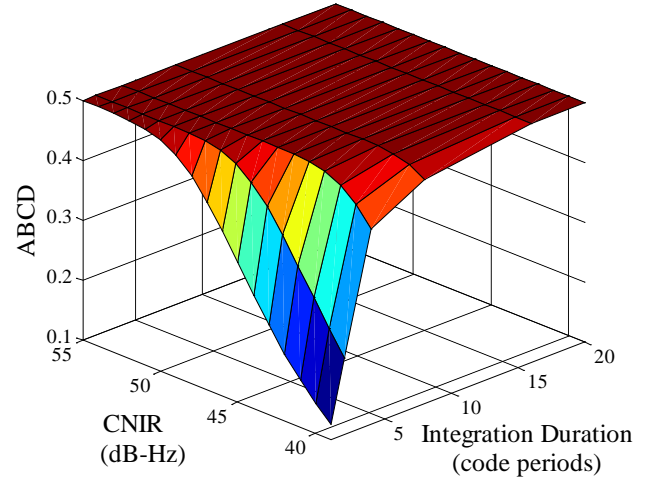


Figure 11: Area between the ROC curves and the diagonal (ABCD) obtained using AA-II algorithm.

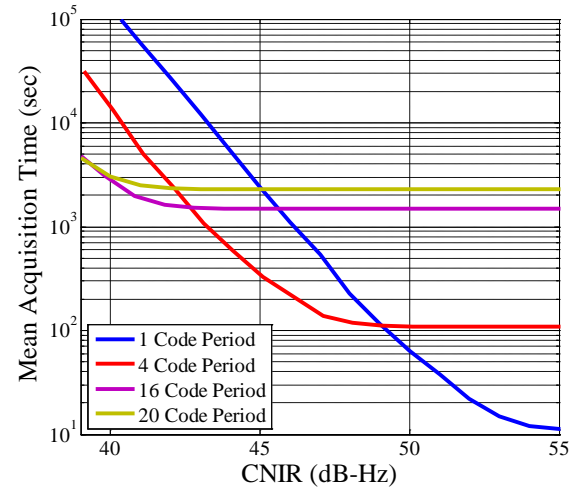


Figure 12: Mean acquisition time achieved using AA-II algorithm for different coherent integration durations.

4. Long Replica Code Acquisition (LRCA)

This section describes an algorithm that simultaneously facilitates coherent integration over multiple code periods, without any assistance (as was required in the case of AA-II) and identifies the SCS index k . The LRCA algorithm employs the hopping (or the slot allocation) sequence elements h_k to generate a matrix H_{RC} :

$$H_{RC} = \begin{bmatrix} h_1 & h_{11} & h_{21} & \cdots & \cdots & h_{191} \\ h_2 & h_{12} & & & & \vdots \\ h_3 & \vdots & \ddots & & & h_{200} \\ \vdots & \vdots & & \ddots & & h_1 \\ \vdots & \vdots & & & \ddots & \vdots \\ h_{20} & h_{30} & \cdots & \cdots & h_{200} & h_{10} \end{bmatrix} \quad (11)$$

Recall that h_k-1 indicated the number of slots between two consecutive SCS: s_k and s_{k+1} . Using elements from the j th column of H_{RC} , a replica code can be generated in the following fashion:

$$R_j = \{C \ Z_{1j} \ C \ Z_{2j} \ C \ \dots \ Z_{20j} \ C\} \quad (12)$$

where C denotes the N_c samples long PRN code and Z denotes a null vector of length $N_z = N_c \times (h_{ij} - 1)$. Here h_{ij} is i th element of the j th column of H_{RC} . Note that each LocataLite transmits its code by gating it in a similar fashion as R_j . The received signal, however, contains the noise (or the undesired PRN signals) instead of zeros. The LRCA algorithm suggests that the received signal, after the carrier is stripped off, to be correlated with each of the 20 replica codes ($R_1 - R_{20}$) generated using columns of H_{RC} . The presence of zeros in the replica code reduces the noise during the correlation process. It can be noted that more than one replica code may either partially or fully match with the received signal, as shown in Figure 13, generating smaller peaks. This is due to the fact that columns used to generate these replica codes may share a number of consecutive elements. The replica code generating the correlation result with the highest peak is selected as the best aligned replica code, considering the fact that this replica code matches the largest number of consecutive SCSs. Also, the position of the peak in the correlation result indicates the phase of the replica code matching with the incoming signal and hence allows the determination of the SCS index. This is possible as the SCS index of each of the slot, as well as the position of that slot in the replica code, is known *a priori*.

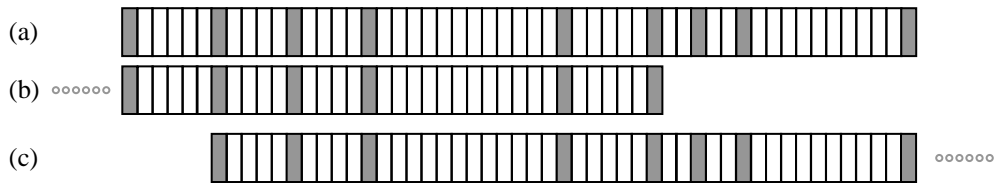


Figure 13 – (a) Positions of SCS in the received signal, (b) Positions of SCS in the replica R_j , (c) Positions of SCS in the replica R_{j+1}

In the case of a received signal with low CNIR, two different replica codes may generate highest peaks of similar strengths. This can be due to the fact that the received noise and interference degrade the peak that

would have otherwise been generated by using the correct clean replica code. In such a scenario the correct column can be identified by extending the length of these replica codes (generating similar peaks) to include the next SCS and selecting the one producing a stronger peak.

In addition, note that the HRC contains columns with the 2nd half of the elements being the same as the first half elements from the next column. This allows that the positions of at least 3/4 of the SCS in the local replica (i.e. 15 SCS) to match those of the received signal. Using H_{RC} with non-overlapping columns, there is a worst case chance that only 10 SCS in the local replica may align with those in the incoming signal and offer lesser coherent integration gain. This can be identified by considering such an H_{RC} given as:

$$H_{RC} = \begin{bmatrix} h_1 & h_{21} & h_{41} & \cdots & \cdots & h_{181} \\ h_2 & h_{22} & & & & \vdots \\ h_3 & \vdots & \ddots & & & \vdots \\ \vdots & \vdots & & \ddots & & \vdots \\ \vdots & \vdots & & & \ddots & \vdots \\ h_{20} & h_{40} & \cdots & \cdots & \cdots & h_{200} \end{bmatrix} \quad (13)$$

The worst case situation will be when the received signal contains SCSs with index $\hat{s}_k - \hat{s}_{k+20}$, where $\hat{s}_k \in \{11, 31, 51, 71, 91, 111, 131, 151, 171, 191\}$. In this case both R_j (column containing \hat{s}_k) and R_{j+1} will have 10 matching SCSs with the received signal. In the case of H_{RC} given by Equation (11), the worst case situation will be when the received signal contains SCS with index $\hat{s}_k - \hat{s}_{k+20}$, where $\hat{s}_k \in \{6, 16, 26, 36, \dots, 186, 196\}$. In this case both R_j and R_{j+1} will have 15 matching SCS with the received signal. The number of worst case matching SCSs can be increased further by increasing the extent of overlap between the columns. However, this will be at the cost of an increase in the number of columns and thus higher computational load.

The same data as used in Section 2.2 was again used to evaluate the performance of the LRCA algorithm. The resulting P_D vs CNIR curve is plotted in Figure 14. It can be seen from this figure that using the LRCA

algorithm, the P_D exceeded the 90% threshold for all CNIR values above 42.8dB-Hz, a gain of 10.7dB over single code period acquisition. Note that this figure also permits comparison of the performance of the LRCA algorithm with other existing (and proposed) acquisition approaches. The existing approaches include signal code period based acquisition and continuous integration, i.e. by integration over entire frames, while the proposed algorithms include non-coherent integration using the PNCA algorithm and coherent integration using assisted acquisition.

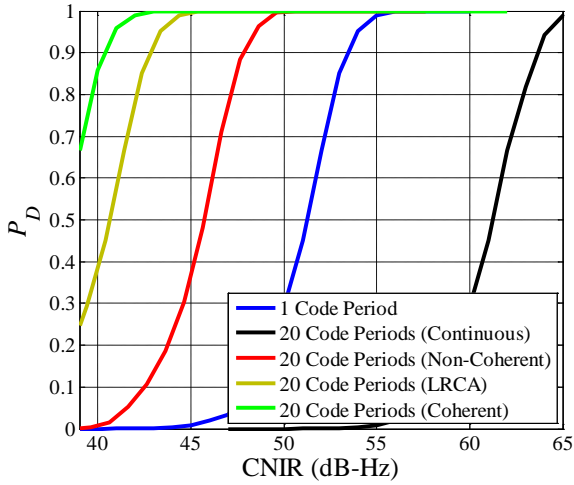


Figure 14: RCA algorithm performance offering coherent integration over single and multiple code periods.

It can be readily noticed that the LRCA algorithm offers significant improvements over single code period integration, 20 code period continuous integration and 20 code period non-coherent integration. However this improvement is less than that offered by coherent integration. Similar observations can be made from the ROC curves plotted in Figure 15, which compare the performance of these algorithms in terms of benefit-to-cost ratios (i.e. P_d/P_{fa}). This was mainly due to the fact that the replica codes may not always fully align with the received signal. A complete alignment of any of the local replica codes with the received signal is a probabilistic event and hence cannot always be guaranteed. It should be noted that in the case where the positions of all the SCSs in the replica code match with those in the received signal, a gain equivalent to that of coherent integration over 20 SCSs is achieved. In the case where not all the SCSs match, the noise contributed by the non-matching SCSs reduces this coherent gain.

Finally, Figure 16 depicts the MAT for the LRCA algorithm. Again, for comparison, the MAT curves for PNCA and AA-II are also plotted here. Note that the curves for only 20 code periods are plotted here for these two algorithms as the LRCA algorithm also considers 20

code periods in the replica codes. It can be seen that the AA-II provides the lowest MAT compared to other algorithms, however this is at the cost of providing assistance data. As compared to the LRCA algorithm, the PNCA algorithm offers low MAT only for mid-to-high CNIR values. LRCA offers lower MAT at lower CNIR values without the need of any assistance data. This particularly helps in situations where no prior acquisitions have been made to obtain the assistance data for using AA-II algorithm.

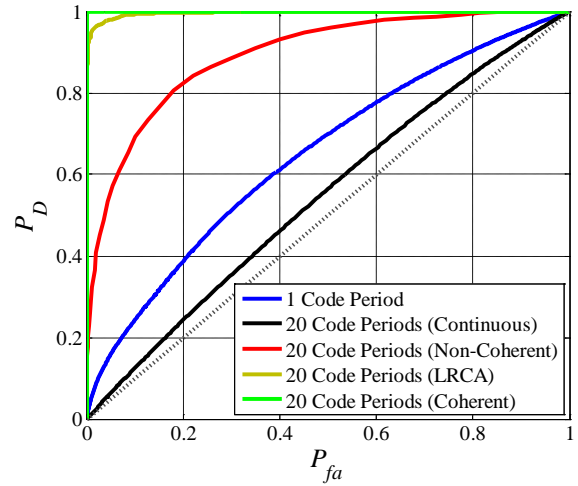


Figure 15: OC curves obtained using AA-II algorithm. Heavy Dotted line shows the diagonal.

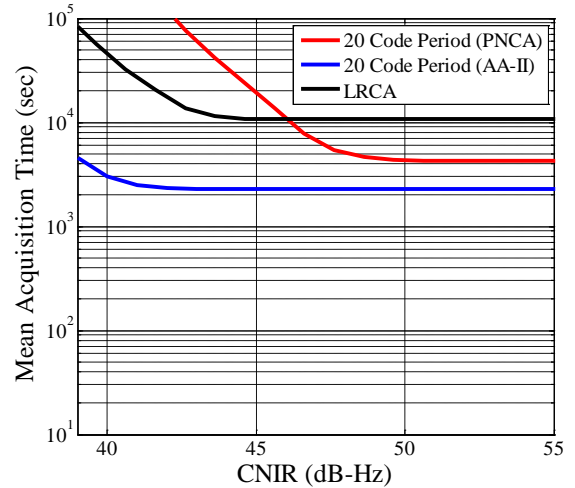


Figure 16: Mean acquisition time for the LRCA algorithm. Results for other algorithms considering same integration durations are also plotted for comparison.

5. Overall Acquisition Strategy:

Employing the proposed acquisition algorithms, an overall acquisition strategy can be summarised as follows:

1. Initiate acquisition for signals from all of the LocataLites using either the PNCA or the LRCA algorithm.
2. As soon as any one of the signals from any of the LocataLites is acquired, determine its SCS index, code start (hence the slot boundary), and the carrier-Doppler.
3. Terminate acquisition of the rest of the signals from the same LocataLite. Instead determine the acquisition parameters for these remaining signals using the AA-I algorithm.
4. Reduce the search space using slot boundary information from step 2 and employ AA-II algorithm for acquiring any one of the signals from each of the remaining LocataLites.
5. Again using the AA-I algorithm, determine acquisition parameters for the rest of the signals from those LocataLites.

If AA-I is employed, only one signal needs to be actually *acquired* for each LocataLite. In case a signal can be identified as the one least affected by the received noise and interference, its acquisition can be prioritised. This will facilitate acquisition using integration over fewer code periods thus reducing computational load and MAT. This identification can be performed by comparing the RMS noise power at each of the two carrier frequencies. This RMS noise power is calculated during acquisitions to set the acquisition threshold by correlating an unused PRN with the received signal. It indicates the potential of noise present (i.e. the extent of signal corruption) at each carrier frequency. This frequency corruption information can then be passed from the initially acquired LocataLite to the rest of the LocataLites for improved acquisitions. However, it needs to be considered that multipath may also contribute to the corruption of a signal at a given frequency, in addition to the possibility of presence of interference at that frequency.

6. Concluding Remarks

This paper has identified the issues involved with Locata signal acquisition under challenging conditions. Locata's use of a pseudorandom gating sequence makes coherent integration exceedingly complex and the non-coherent integration is also more complicated than in case of GNSS. Four algorithms were proposed to address the situation. Real Locata signals were used to evaluate the performance of these proposed algorithms and to quantify the receiver sensitivity improvement that could be achieved. It was shown that the probabilistic positions of desired SCSs can be used to perform non-coherent integration beyond single code period for improved acquisition. Implementation results suggest that this non-coherent integration offers an improvement margin of 1.3dB after experiencing loss due to squaring and the ambiguity involved in the considered SCS position. It

was also demonstrated that this margin can be improved by obtaining assistance data from any of the previously acquired signals. A concept of assisted acquisition was introduced and it was shown that this offers an additional margin of 1.7dB with reduction in the computational load. Results were presented which suggest that the assisted acquisition offers faster acquisition of low CNIR signals. In addition, the use of long replica codes was suggested and it was shown that this allows coherent integration without requiring any assistance.

The work reported in this paper suggests the following trade-offs exist among the proposed schemes:

- Continuous integration over multiple code periods can be performed with least computational load but accumulates more noise than the desired signal and performs poorly for increased integration durations.
- The PNCA algorithm allows non-coherent integration over multiple code periods offering sensitivity improvement and does not require any assistance data.
- Alternatively, assisted acquisition, using assistance information from previous successful acquisitions, offers better sensitivity improvement with minimum computational load as well as MAT.
- The LRCA algorithm requires increased acquisition times but significantly outperforms the PNCA algorithm and does not require any assistance data.

An overall acquisition strategy was proposed that suggests the sequence in which these proposed algorithms can be used to reduce overall computational load, lower the mean acquisition time and improve receiver sensitivity.

Acknowledgement

This research is supported by Australian Research Council Linkage Projects LP0668907 and LP0560910.

References

- Barnes, J., C. Rizos, J. Wang, D. Small, G. Voight, and N. Gambale (2003) *Locatanet: The positioning technology of the future?* 6th Int. Symp. on Satellite Navigation Technology Including Mobile Positioning & Location Services, Melbourne, Australia, 22-25 July, CD-ROM proc., paper 49.
- Borio, D., C. O'Driscoll, G. Lachapelle (2008), *Composite GNSS signal acquisition over multiple code periods*. IEEE Transactions on Aerospace & Electronic Systems, 46(1), 193-206.
- Borre, K., D.M. Akos, N. Bertelsen, P. Rinder and S.H. Jensen (2007) *A Software-Defined GPS and Galileo Receiver: A Single-Frequency Approach*. Birkhäuser Boston.

- Cheong, J.W., X. Wei, N. Politi, A.G. Dempster and C. Rizos (2009a) *Characterising the signal structure of Locata's pseudolite-based positioning system*. IGNSS Symp., Gold Coast, Australia, 1-3 December, CD-ROM procs.
- Cheong, J.W., A.G. Dempster and C. Rizos (2009b) *Detection of time-hopped DS-CDMA signal for pseudolite-based positioning system*. 22nd Int. Tech. Meeting of the Satellite Division of the U.S. Inst. of Navigation, Savannah, Georgia, USA, 22-25 September, 881-891.
- Cheong, J.W., F.A. Khan, A.G. Dempster and C. Rizos (2010) *Locata system and signal architecture*. Internal Document, SPRINT Group, University of New South Wales.
- Cobb, S.H. (1997) *GPS Pseudolites: Theory, Design and Applications*, Doctoral Dissertation, Stanford University.
- Hanley, J.A., and B.J. McNeil (1982) *The meaning and use of the area under a receiver operating characteristic (ROC) curve*. Radiology, 143, 29-36.
- Kaplan, E.D., Hegarty, C.J. (2006) *Understanding GPS: Principles and Applications*, Second Edition, Artech House, Norwood, MA, 726pp.
- Khan, F.A., A.G. Dempster and C. Rizos (2010) *Locata performance evaluation in the presence of wide- and narrow-band interference*. Journal of Navigation, Royal Institute of Navigation, 63(3), 527-543.

Biography

Faisal Ahmed Khan is currently a doctoral candidate at the School of Surveying & Spatial Information Systems, University of New South Wales (UNSW). His main area of research is interference effects analysis and mitigation. He holds a M.Phil. degree from UNSW, Australia, and a B.E. (Electronics) degree from NED UET, Pakistan. He has also gained hands-on experience in the field of satellite communications at Institute of Space Technology and the Pakistan Space and Upper Atmosphere Research Commission.